

Deterministic Nonlocal Quantum Gate with Room-Temperature Memory ModulesXing Lei^{1,*}, Jiatong Li^{1,*}, Xiaoyu Zhou,¹ Jieli Yan¹, Minwen Ji,¹ Zhihui Yan^{1,2,†}, Xiaojun Jia,^{1,2,‡}
Changde Xie,^{1,2} and Kunchi Peng^{1,2}¹*State Key Laboratory of Quantum Optics Technologies and Devices,**Institute of Opto-Electronics, Shanxi University, Taiyuan, 030006, People's Republic of China*²*Collaborative Innovation Center of Extreme Optics, Shanxi University, Taiyuan 030006, People's Republic of China*

(Received 3 March 2025; accepted 4 September 2025; published 25 September 2025)

Scaling quantum computation is a crucial challenge for practical applications, hindered by the inherent errors and noises in real-world quantum systems. The quantum modular architecture offers a possible solution, where smaller quantum modules are individually constructed and assembled into a larger architecture. In this architecture, the nonlocal quantum gates are the building blocks; until now, it has remained challenging for practical applications to implement a nonlocal quantum gate with the memory modules under deterministic and room-temperature conditions, due to intrinsic probability and hardware complexity. Here, we propose and demonstrate a scheme to deterministically implement a nonlocal quantum gate between the room-temperature memory modules. The key technologies include cavity-enhanced atomic modules, two of which are connected by a single pair of distributed entangled optical modes and real-time mutual feedforward controls. The nonlocal quantum nondemolition gate between two room-temperature memory modules is deterministically demonstrated with different input coherent states, and the quantum nature is confirmed by outputting entangled atomic modules. Our results illustrate the functionality and feasibility of nonlocal quantum gate and may have potential applications in modular quantum information processing.

DOI: [10.1103/xt77-2gpw](https://doi.org/10.1103/xt77-2gpw)

Quantum computation with exponential computational power can solve problems that cannot be dealt with the classical approach. In the past decades, the computational advantages for a particular task have been dramatically enhanced by exploring quantum resources [1–3]. The scalability of quantum computation is key for computational power [4,5]; nevertheless, it is limited by unavoidable errors and noises, which disturb fragile quantum states and quantum operations. To address these challenges, fault-tolerant quantum error correction can significantly improve its scalability, where multiple physical qubits are combined into a logical qubit for robustly preserving quantum information [6–9]. Particularly, quantum modular architecture can build complex quantum systems robustly by connecting small distributed modules into a quantum network [10–12]. Quantum modules, capable of storing and processing quantum information, operate individually as functional nodes and enable the high-quality quantum operations inside each module. Even in a large-scale quantum network, each module is well isolated from every other module, so that the residual interactions across the entire network are minimized. Thus, it is highly demanded

to realize the nonlocal quantum gate across spatially separated modules, which makes the computation capacity greatly enhanced [13,14].

Quantum networks play a significant role in enhancing the scalability of quantum information processing by interconnecting quantum modules [15,16]. Quantum nodes are employed to process quantum information, while the flying optical modes through quantum channels can coherently connect quantum nodes and transfer quantum information. Quantum entanglement constitutes the building block of quantum network [17,18] and has been established and stored in a variety of physical systems ranging from neutral atoms [19,20] and trapped ions [21–23] to superconductors [24,25] and solid systems [26,27]. If the entanglement of light is mapped into the atomic ensembles, these ensembles can be entangled [28–30]. Beyond the capability to generate and store quantum entanglement in quantum nodes, the ability to implement nonlocal quantum gate is a pivotal step for modular quantum architecture [31,32]. Photonics offers a promising distant and reconfigurable platform for a larger-scale quantum computation, where photonic quantum modules with a relatively small number of quantum states are interconnected [33]. Extensive efforts on the photonic nonlocal quantum gates have been achieved in different kinds of physical platforms based on quantum entanglement between cryogenically cooled crystals, laser-cooled atoms, and ions [34–36].

*These authors contributed equally to this work.

†Contact author: zhyan@sxu.edu.cn

‡Contact author: jiaxj@sxu.edu.cn

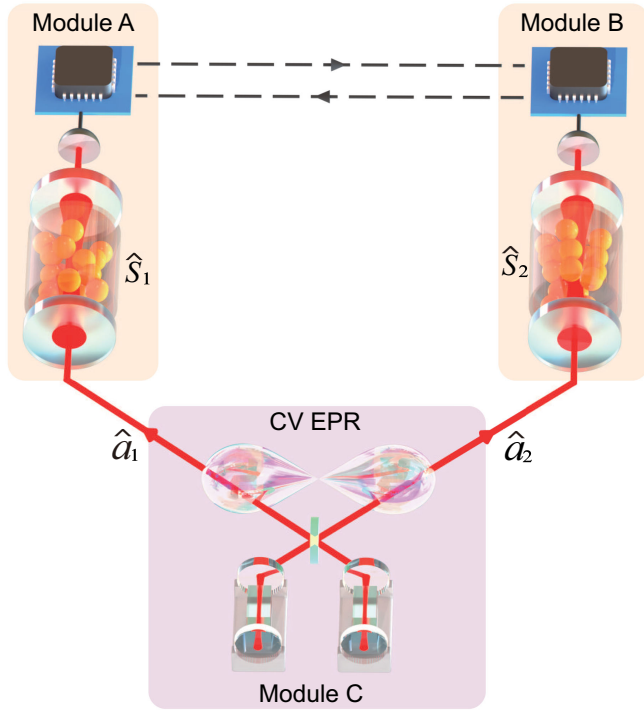


FIG. 1. Schematic diagram of the deterministic nonlocal quantum gate between spatially separated room-temperature quantum memory modules. Quantum modules *A* and *B* are two cavity-enhanced atomic modules at room temperature to process and store quantum information. Quantum module *C* is the quantum resource to deterministically generate a pair of CV EPR entangled optical modes (solid lines), which are distributed to connect two atomic modules. The nonlocal quantum gate is implemented by real-time mutual feedforward control with the BHD results via classical communication channels (dashed lines).

Nevertheless, it remains challenging to deterministically execute a nonlocal quantum gate across room-temperature quantum memory modules, which is essential for the scalable quantum modular architecture.

Here, we design and demonstrate a nonlocal quantum gate between memory modules with a spatial separation of 3 m, which operates under deterministic and room-temperature conditions. We develop two sets of cavity-enhanced atomic modules, which are interconnected by a single pair of distributed entangled optical modes and real-time mutual feedforward controls. Both functions of quantum gate and quantum memory can be realized in this system, which consists of three quantum modules in Fig. 1. A logical quantum mode is encoded in the conjugate quadrature components of the collective atomic spin waves in quantum modules *A* and *B*. First, two sets of cavity-enhanced atomic modules with birefringent crystals are developed as control and target modules for processing and storing quantum information. The room-temperature atomic cells offer an attractive physical system with advantages featuring strong and controlled interaction and simple operation [37–39] and can be explored for quantum memory of optical

quantum states [29,40,41]. However, there is a trade-off between the memory temperature and noise in atomic cells. With the cavity-enhanced technique [42], the memory cavity with birefringent material suppresses noise by the perfect cavity antiresonance, while the memory cavity enables strong interaction by cavity resonance with the signal and control beams. Thus, cavity-enhanced quantum memory with birefringent material makes room-temperature operation feasible. Second, continuous-variable (CV) Einstein-Podolsky-Rosen (EPR) entangled modes are deterministically generated in module *C* and distributed to connect two spatially separated modules *A* and *B*. The CV quantum information paves an effective avenue for deterministically generating, manipulating, and detecting quantum states [43–45]. Quantum memory for CV entangled modes has been achieved in room-temperature atomic modules [30,46], which is the building block of quantum gate. In our scheme, the submodes of EPR state (\hat{a}_1 and \hat{a}_2) are generated by two optical parametric amplifiers with a beam splitter and are distributed to two spatially separated modules with the atomic spin wave (\hat{S}_1 and \hat{S}_2). Third, the real-time mutual feedforward controls are developed to implement a nonlocal quantum non-demolition (QND) gate [47]. The measurement-based feedforward is utilized for quantum operations across spatially separated atomic modules and offers an ideal interface to avoid the unrecoverable loss of quantum information during transfer across quantum channels [48]. With real-time mutual feedforward controls, the nonlocal QND gate is deterministically implemented. The quantum state in one module can be changed on the basis of the quantum state in the other one, and the genuine quantum nature of the gate is verified by deterministically entangling these two output atomic modules. Therefore, this system not only deterministically achieves nonlocal quantum gate between room-temperature memory modules, but also significantly decreases the hardware cost and simplifies the complexity of scalable quantum networks.

To achieve such a nonlocal quantum gate, a quantum network architecture is developed to address all aspects including the quantum source, distribution modules, and mutual classical controls. The aim of nonlocal QND gate between quantum nodes is to realize controlled-NOT operation for the target state with the help of the control state. For CV systems, the basic units of quantum information are quantum modes, instead of quantum bits in discrete variable systems, and an equivalent of the basic controlled-NOT gate for quantum bit systems is a QND gate for quantum mode systems ($\sum_{AB} |a\rangle_A |b\rangle_B = |a\rangle_A |a+b\rangle_B$, $a, b \in R$) [49,50]. The QND gate is implemented between two nonlocal atomic modules interconnected by a pair of distributed entangled modes. The input states of the modules are coupled with the shared EPR state based on the light-atom interference. Subsequently, the balanced homodyne detection (BHD) of transmitted modes on each module make the projection on

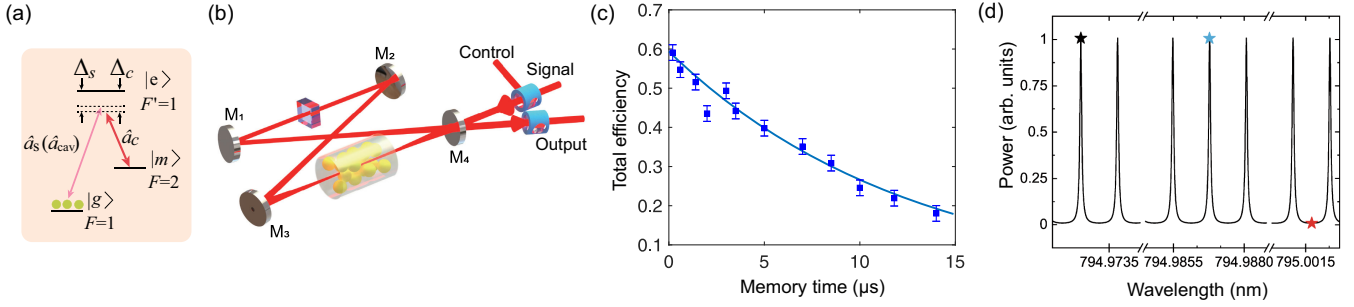


FIG. 2. Performances of the room-temperature memory module. (a) The atomic energy levels for the quantum module. (b) Experimental setup of the cavity-enhanced quantum module. (c) The dependence of the total efficiency on memory time. (d) Noise suppression effect of the memory cavity. The black star represents the signal mode resonant with the cavity; the blue star represents the control mode resonant with the cavity; and the red star represents the four-wave mixing noise antiresonant with the cavity.

the eigenstate of either amplitude or phase quadratures. Finally, a nonlocal QND gate between cavity-enhanced atomic modules is deterministically realized with the aid of entangled optical modes and real-time mutual feedforward controls in a two-way architecture between modules *A* and *B* (see Supplemental Material [51] for the detailed experimental setup).

The quantum memory is achieved in room-temperature quantum modules *A* and *B*, where the electromagnetically induced transparency in a three-level atomic system is employed in Fig. 2(a). The cavity-enhanced atomic module consists of an atomic cell, an optical cavity, and a birefringent crystal shown in Fig. 2(b), which is key for processing quantum states with high fidelity. When the collective atomic spin wave $\hat{S}(t)$ interacts with the signal mode $\hat{a}(t)$ via effective light-atom interaction constant κ , the quantum states of the signal mode and the atomic ensemble can be reversibly transferred, owing to the beam splitter interaction of Hamiltonian $\hat{H} = \kappa \hat{a}_j^\dagger \hat{S}_j + \text{H.c.}$ ($j \in 1, 2$) [61]. The total efficiency is defined as the ratio between the energies of the released signal mode and the input signal mode, which is the product of the write-in and readout efficiency, and can be directly measured by a detector. The dependence of the total efficiency on memory time is shown in Fig. 2(c). The total efficiency can reach 0.60 with a storage time of 500 ns, and the maximum storage lifetime is 10 μs . The noise suppression effect is characterized by the power in cavity shown as Fig. 2(d). The noise suppression factor with the birefringent crystal is enhanced to 0.10 compared with that of 0.24 without the birefringent crystal and can reach the limit of 0.02 (see Supplemental Material [51] for the quantum memory details).

With such high-performance quantum modules, a nonlocal QND gate is deterministically realized with quantum module *C*, where the parametric amplification in the cavity is widely used as quantum source module for connecting quantum modules *A* and *B*. The Hamiltonian of the quantum source is a parametric amplification-type interaction, expressed as $\hat{H}_L = \chi \hat{a}_j^\dagger \hat{a}_j^\dagger + \text{H.c.}$ ($j \in 1, 2$) with a nonlinear coefficient χ . A pair

of CV Einstein-Podolsky-Rosen entangled optical modes are generated by coupling two squeezed states from two optical parametric amplifiers on a beam splitter. The amplitude and phase quadratures of their submodes are, respectively, $\hat{x}_j = \hat{a}_j + \hat{a}_j^\dagger$ and $\hat{p}_j = (\hat{a}_j - \hat{a}_j^\dagger)/i$ ($j \in 1, 2$), and the quadrature correlation variances with squeezing parameter r are $\delta^2(\hat{x}_1 - \hat{x}_2) = \delta^2(\hat{p}_1 + \hat{p}_2) = 2e^{-2r}$, where the squeezed parameter of 0.35 at the rubidium D_1 line is used.

By using mutual feedforward controls, the nonlocal quantum gate is deterministically realized, and the output quadratures of one atomic module depend on the other one. The amplitude and phase quadratures of distributed entangled optical modes can be mapped to the quadratures of atomic spin wave in quantum modules, $\hat{X}_j = \hat{S} + \hat{S}^\dagger$ and $\hat{P}_j = (\hat{S} - \hat{S}^\dagger)/i$ ($j \in 1, 2$). The nonlocal QND gate between memory modules is encoded in the amplitude and phase quadratures of quantum modules. In the ideal case, the output amplitude and phase quadratures of quantum modules are

$$\begin{pmatrix} \hat{X}_1^O \\ \hat{P}_1^O \\ \hat{X}_2^O \\ \hat{P}_2^O \end{pmatrix} = \begin{pmatrix} \sqrt{2}\hat{X}_1^0 \\ \frac{1}{\sqrt{2}}\hat{P}_1^0 - \frac{1}{\sqrt{2}}\hat{P}_2^0 \\ \frac{1}{\sqrt{2}}\hat{X}_2^0 + \frac{1}{\sqrt{2}}\hat{X}_1^0 \\ \sqrt{2}\hat{P}_2^0 \end{pmatrix}, \quad (1)$$

where $\hat{X}_{1(2)}^0$ and $\hat{P}_{1(2)}^0$ are the amplitude and phase quadratures, respectively, of the initial quantum state. The calculation details of the quadrature variances in the actual case are given in Supplemental Material Note III [51]. To test the universal input-output relations of the QND gate, the vacuum state and the four different coherent states are used as input states. The covariance matrix for Gaussian states can completely describe the QND gate output state, and the measurement results of the corresponding output covariance matrixes with different input states are demonstrated in Figs. 3(a)–3(e), respectively. Figure 3(a) shows the output noise variances of the quadratures \hat{X}_1^O , \hat{X}_2^O , \hat{P}_1^O ,

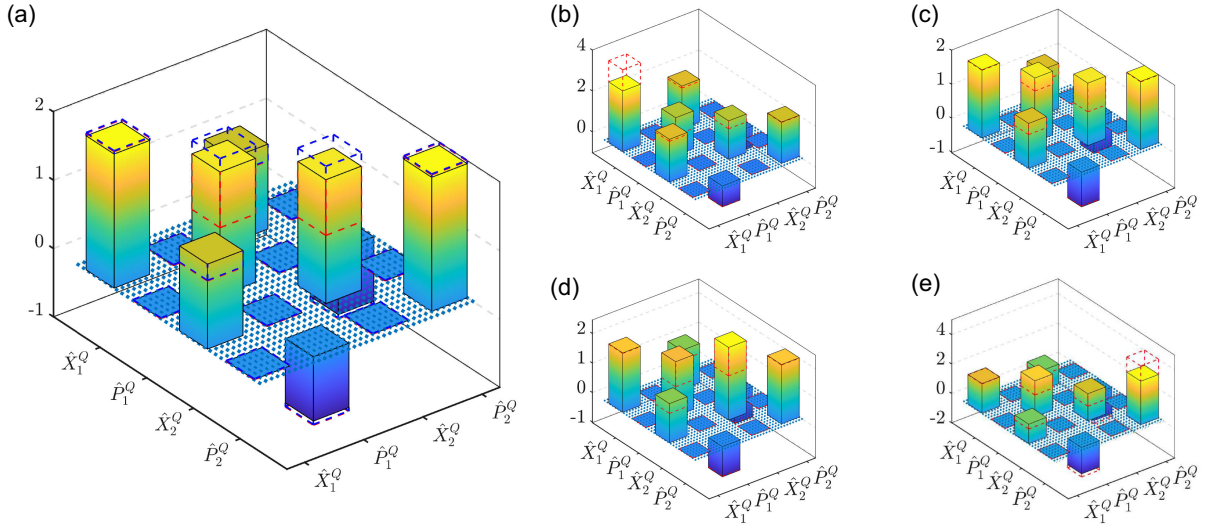


FIG. 3. Covariance matrices of the deterministic nonlocal QND gate output states. (a) Covariance matrices of the output states (\hat{X}_1^Q , \hat{X}_2^Q , \hat{P}_1^Q , and \hat{P}_2^Q) for vacuum input states. (b)–(e) Covariance matrices of the output states for four different coherent input states (\hat{X}_1^0 , \hat{X}_2^0 , \hat{P}_1^0 , and \hat{P}_2^0) with displacements of vacuum noise, respectively. The output states marked with red and blue dashed lines correspond to $r = \infty$ and $r = 0$, respectively.

and \hat{P}_2^Q of the quantum modules A and B with a vacuum input mode. In the ideal case, the output variances of \hat{X}_1^Q and \hat{P}_2^Q are 3.0 dB above the shot-noise level (SNL), while the output variances of \hat{X}_2^Q and \hat{P}_1^Q are at the level of SNL, due to the effect of QND gate [see Eq. (1)]. The ideal performance is marked by the red lines, and the deviation from the actual measured noise variances is caused by finite squeezing and mapping efficiency. The blue lines stand for the output noises with a coherent state instead of the entangled state, and the variances of \hat{X}_1^Q , \hat{P}_1^Q , \hat{X}_2^Q , and \hat{P}_2^Q are both 3.0 dB above the SNL. In experiment, the variances of \hat{X}_1^Q (\hat{P}_2^Q) and \hat{X}_2^Q (\hat{P}_1^Q) measured with the entangled modes are 2.9 and 2.6 dB above the SNL, respectively. Figures 3(b)–3(e) demonstrate the measurement results of the corresponding output covariance matrices with four different coherent states \hat{X}_1^0 , \hat{X}_2^0 , \hat{P}_1^0 , and \hat{P}_2^0 . The output quadratures \hat{X}_1^Q and \hat{P}_2^Q depend only on the single module. The output quadratures \hat{P}_1^Q and \hat{X}_2^Q are controlled by the quadratures of the other modules \hat{P}_2^0 and \hat{X}_1^0 , respectively, where the uncorrelated quantum fluctuations of \hat{P}_2^0 and \hat{X}_1^0 are added to those of \hat{P}_1^0 and \hat{X}_2^0 , respectively.

Notably, the QND gate is confirmed by checking the entanglement between the output states, which can be verified using the positivity under the positive partial transposition criterion [62,63]. If the value of the minimum symplectic eigenvalue E is less than the benchmark of unity, the QND gate can create the entangled atomic modules from two pure separable states, when the initial quantum states owned by these modules are the coherent states. To analyze the entanglement of the QND gate output state, the

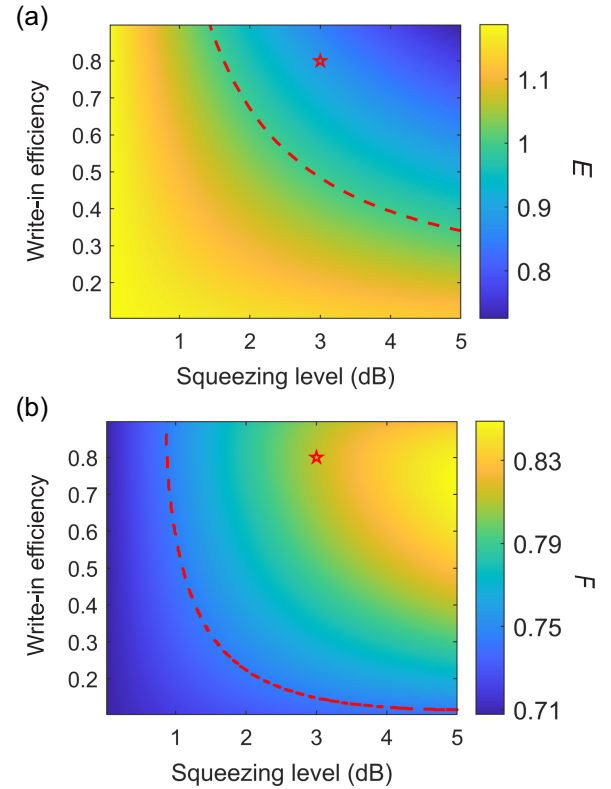


FIG. 4. Characterizations of the deterministic nonlocal QND gate. Minimum symplectic eigenvalue E (a) and fidelity F (b) of nonlocal QND gate output states versus the input squeezing level of the optical mode and write-in efficiency of quantum memory, respectively. The red dashed lines correspond to coherent states. The red stars are the experimental point.

dependence of the minimum symplectic eigenvalue E on the input squeezing level of the optical mode and the write-in efficiency of the atomic module is as illustrated in Fig. 4(a). Entanglement can be achieved within the upper boundary region indicated by the red line, and the minimum symplectic eigenvalue E can be optimized by enhancing the total efficiency and optical transmission efficiency. In the experiment, the minimum symplectic eigenvalue E in the atomic ensemble reaches 0.80 ± 0.08 with normalization (corresponding to 0.94 ± 0.10 of the released optical modes), when the input squeezing level is 3.0 ± 0.1 dB, and a write-in efficiency of 0.80 ± 0.01 is experimentally used. These results show the output states form an entangled state between these two atomic modules and characterize the quantum logical process.

Furthermore, the fidelity describes the overlap between the experimental output state $\hat{\rho}_e$ and the ideal output state $\hat{\rho}_i$ and quantifies the performance of the QND gate. Figure 4(b) shows the function of fidelity on the input squeezing level of the optical mode and the write-in efficiency of the atomic module. The optimal write-in efficiency and higher squeezing level are required for fidelity. The experimental fidelity of 0.81 ± 0.06 is achieved as the red star, and the theoretical limit can reach 0.88, when the fidelity is 0.75 with the coherent state. Thus, a nonlocal QND gate can be deterministically realized in such a quantum network, which demonstrates its functionalities of quantum gate and memory as well as feasibility of room-temperature operation. Furthermore, the fidelity of the nonlocal QND gate can be improved by the enhancement of squeezing levels and total efficiency, reductions of memory noise, and optical transmission losses, besides noiseless linear amplification (see Supplemental Material [51] for the QND gate calculation details).

In summary, we have simultaneously realized deterministic quantum gate and memory with spatially separated room-temperature modules while minimizing the cost of quantum hardware and simplifying the complexity of quantum networks. With distributed a pair of entangled optical modes and mutual feedforward control, the nonlocal QND gate with storage capability is deterministically realized between cavity-enhanced atomic modules. Moreover, our implementation can be adapted in the future to incorporate schemes for frequency conversion and commercial optical fibers [64–66] and enables quantum networks with more modules to implement complex quantum operations by using multipartite entanglement [67,68]. This resource-efficient quantum network overcomes the deterministic and room-temperature operation challenges of scalable modular quantum processors and may offer an efficient way toward distributed quantum networks [69].

Acknowledgments—The work was supported by the Innovation Program for Quantum Science and Technology (Grant No. 2024ZD0300900), the Key Project of the National Key R&D program of China

(Grant No. 2022YFA1404500), the National Natural Science Foundation of China (Grants No. 62122044, No. 61925503, and No. 62135008), the Fundamental Research Program of Shanxi Province (Grant No. 202403021223001), and the fund for Shanxi “1331 Project” Key Subjects Construction.

Data availability—The data that support the findings of this article are not publicly available. The data are available from the authors upon reasonable request.

-
- [1] T. D. Ladd, F. Jelezko, R. Laflamme, Y. Nakamura, C. Monroe, and J. L. O’Brien, Quantum computers, *Nature (London)* **464**, 45 (2010).
 - [2] F. Arute *et al.*, Quantum supremacy using a programmable superconducting processor, *Nature (London)* **574**, 505 (2019).
 - [3] H.-S. Zhong *et al.*, Quantum computational advantage using photons, *Science* **370**, 1460 (2020).
 - [4] M. V. Larsen, X. Guo, C. R. Breum, J. S. Neergaard-Nielsen, and U. L. Andersen, Deterministic multi-mode gates on a scalable photonic quantum computing platform, *Nat. Phys.* **17**, 1018 (2021).
 - [5] L. S. Madsen *et al.*, Quantum computational advantage with a programmable photonic processor, *Nature (London)* **606**, 75 (2022).
 - [6] B. M. Terhal, Quantum error correction for quantum memories, *Rev. Mod. Phys.* **87**, 307 (2015).
 - [7] C. Figgatt, A. Ostrander, N. M. Linke, K. A. Landsman, D. Zhu, D. Maslov, and C. Monroe, Parallel entangling operations on a universal ion-trap quantum computer, *Nature (London)* **572**, 368 (2019).
 - [8] S. Konno *et al.*, Logical states for fault-tolerant quantum computation with propagating light, *Science* **383**, 289 (2024).
 - [9] D. Bluvstein *et al.*, Logical quantum processor based on reconfigurable atom arrays, *Nature (London)* **626**, 58 (2024).
 - [10] N. H. Nickerson, Y. Li, and S. C. Benjamin, Topological quantum computing with a very noisy network and local error rates approaching one percent, *Nat. Commun.* **4**, 1756 (2013).
 - [11] C. Monroe, R. Raussendorf, A. Ruthven, K. R. Brown, P. Maunz, L. M. Duan, and J. Kim, Large-scale modular quantum-computer architecture with atomic memory and photonic interconnects, *Phys. Rev. A* **89**, 022317 (2014).
 - [12] Y. Li and J. D. Thompson, High-rate and high-fidelity modular interconnects between neutral atom quantum processors, *PRX Quantum* **5**, 020363 (2024).
 - [13] B. Jing *et al.*, Entanglement of three quantum memories via interference of three single photons, *Nat. Photonics* **13**, 210 (2019).
 - [14] Y. Zhong *et al.*, Deterministic multi-qubit entanglement in a quantum network, *Nature (London)* **590**, 571 (2021).
 - [15] H. J. Kimble, The quantum internet, *Nature (London)* **453**, 1023 (2008).
 - [16] S. Wehner, D. Elkouss, and R. Hanson, Quantum internet: A vision for the road ahead, *Science* **362**, eaam9288 (2018).

- [17] S. Liang, J. Cheng, J. Qin, J. Li, Y. Shi, Z. Yan, X. Jia, C. Xie, and K. Peng, High-speed quantum radio-frequency-over-light communication, *Phys. Rev. Lett.* **132**, 140802 (2024).
- [18] Z. Yan and X. Jia, Quantum key distribution with chromatic codes, *Light Sci. Appl.* **14**, 126 (2025).
- [19] T. van Leent *et al.*, Entangling single atoms over 33 km telecom fibre, *Nature (London)* **607**, 69 (2022).
- [20] J. L. Liu *et al.*, Creation of memory–memory entanglement in a metropolitan quantum network, *Nature (London)* **629**, 579 (2024).
- [21] V. Krutyanskiy *et al.*, Entanglement of trapped-ion qubits separated by 230 meters, *Phys. Rev. Lett.* **130**, 050803 (2023).
- [22] S. Saha, M. Shalaev, J. O’Reilly, I. Goetting, G. Toh, A. Kalakuntla, Y. Yu, and Christopher Monroe, High-fidelity remote entanglement of trapped atoms mediated by time-bin photons, *Nat. Commun.* **16**, 2533 (2025).
- [23] C. Wang, C. Huang, H. Zhang, H. Hu, Z. Mao, P. Hou, Y. Wu, Z. Zhou, and L. Duan, Experimental realization of direct entangling gates between dual-type qubits, *Phys. Rev. Lett.* **134**, 010601 (2025).
- [24] P. Kurpiers *et al.*, Deterministic quantum state transfer and remote entanglement using microwave photons, *Nature (London)* **558**, 264 (2018).
- [25] J. Grebel *et al.*, Bidirectional multiphoton communication between remote superconducting nodes, *Phys. Rev. Lett.* **132**, 047001 (2024).
- [26] C. M. Knaut *et al.*, Entanglement of nanophotonic quantum memory nodes in a telecom network, *Nature (London)* **629**, 573 (2024).
- [27] A. Ruskuc, C.-J. Wu, E. Green, S. L. N. Hermans, W. Pajak, J. Choi, and A. Faraon, Multiplexed entanglement of multi-emitter quantum network nodes, *Nature (London)* **639**, 54 (2025).
- [28] K. S. Choi, H. Deng, J. Laurat, and H. J. Kimble, Mapping photonic entanglement into and out of a quantum memory, *Nature (London)* **452**, 67 (2008).
- [29] K. Jensen, W. Wasilewski, H. Krauter, T. Fernholz, B. M. Nielsen, M. Owari, M. B. Plenio, A. Serafini, M. M. Wolf, and E. S. Polzik, Quantum memory for entangled continuous-variable states, *Nat. Phys.* **7**, 13 (2011).
- [30] Z. Yan, L. Wu, X. Jia, Y. Liu, R. Deng, S. Li, H. Wang, C. Xie, and K. Peng, Establishing and storing of deterministic quantum entanglement among three distant atomic ensembles, *Nat. Commun.* **8**, 718 (2017).
- [31] A. Reiserer and G. Rempe, Cavity-based quantum networks with single atoms and optical photons, *Rev. Mod. Phys.* **87**, 1379 (2015).
- [32] J. Niu *et al.*, Demonstrating path-independent anyonic braiding on a modular superconducting quantum processor, *Phys. Rev. Lett.* **132**, 020601 (2024).
- [33] H. Aghaee Rad *et al.*, Scaling and networking a modular photonic quantum computer, *Nature (London)* **638**, 912 (2025).
- [34] S. Daiss, S. Langenfeld, S. Welte, E. Distant, P. Thomas, L. Hartung, O. Morin, and G. Rempe, A quantum-logic gate between distant quantum-network modules, *Science* **371**, 614 (2021).
- [35] X. Liu *et al.*, Nonlocal photonic quantum gates over 7.0 km, *Nat. Commun.* **15**, 8529 (2024).
- [36] D. Main, P. Drmota, D. P. Nadlinger, E. M. Ainley, A. Agrawal, B. C. Nichol, R. Srinivas, G. Araneda, and D. M. Lucas, Distributed quantum computing across an optical network link, *Nature (London)* **638**, 383 (2025).
- [37] J. Guo, X. Feng, P. Yang, Z. Yu, L. Q. Chen, C.-H. Yuan, and W. Zhang, High-performance raman quantum memory with optimal control in room temperature atoms, *Nat. Commun.* **10**, 148 (2019).
- [38] H. Bao *et al.*, Spin squeezing of 10^{11} atoms by prediction and retrodiction measurements, *Nature (London)* **581**, 159 (2020).
- [39] S. Liu, Y. Lv, X. Wang, J. Wang, Y. Lou, and J. Jing, Deterministic all-optical quantum teleportation of four degrees of freedom, *Phys. Rev. Lett.* **132**, 100801 (2024).
- [40] J. Appel, E. Figueroa, D. Korystov, M. Lobino, and A. I. Lvovsky, Quantum memory for squeezed light, *Phys. Rev. Lett.* **100**, 093602 (2008).
- [41] K. Honda, D. Akamatsu, M. Arikawa, Y. Yokoi, K. Akiba, S. Nagatsuka, T. Tanimura, A. Furusawa, and M. Kozuma, Storage and retrieval of a squeezed vacuum, *Phys. Rev. Lett.* **100**, 093601 (2008).
- [42] D. J. Saunders, J. H. D. Munns, T. F. M. Champion, C. Qiu, K. T. Kaczmarek, E. Poem, P. M. Ledingham, I. A. Walmsley, and J. Nunn, Cavity-enhanced room-temperature broadband raman memory, *Phys. Rev. Lett.* **116**, 090501 (2016).
- [43] X. Zuo, Z. Yan, Y. Feng, J. Ma, X. Jia, C. Xie, and K. Peng, Quantum interferometer combining squeezing and parametric amplification, *Phys. Rev. Lett.* **124**, 173602 (2020).
- [44] C. Fabre and N. Treps, Modes and states in quantum optics, *Rev. Mod. Phys.* **92**, 035005 (2020).
- [45] J. Cheng, S. Liang, J. Qin, J. Li, Z. Yan, X. Jia, C. Xie, and K. Peng, Semi-device-independent quantum random number generator with a broadband squeezed state of light, *npj Quantum Inf.* **10**, 20 (2024).
- [46] H. Krauter, C. A. Muschik, K. Jensen, W. Wasilewski, J. M. Petersen, J. I. Cirac, and E. S. Polzik, Entanglement generated by dissipation and steady state entanglement of two macroscopic objects, *Phys. Rev. Lett.* **107**, 080503 (2011).
- [47] S. Yokoyama, R. Ukai, J. I. Yoshikawa, P. Marek, R. Filip, and A. Furusawa, Nonlocal quantum gate on quantum continuous variables with minimal resources, *Phys. Rev. A* **90**, 012311 (2014).
- [48] R. Raussendorf and H. J. Briegel, A one-way quantum computer, *Phys. Rev. Lett.* **86**, 5188 (2001).
- [49] J. Eisert, K. Jacobs, P. Papadopoulos, and M. B. Plenio, Optimal local implementation of nonlocal quantum gates, *Phys. Rev. A* **62**, 052317 (2000).
- [50] R. Filip, Continuous-variable quantum nondemolishing interaction at a distance, *Phys. Rev. A* **69**, 052313 (2004).
- [51] See Supplemental Material at <http://link.aps.org/supplemental/10.1103/xt77-2gpw>, which includes Refs. [52–60], for additional information about the calculation details and the experimental setup.
- [52] H. Krauter, D. Salart, C. A. Muschik, J. M. Petersen, H. Shen, T. Fernholz, and E. S. Polzik, Deterministic quantum teleportation between distant atomic objects, *Nat. Phys.* **9**, 400 (2013).
- [53] D. V. Sychev, A. E. Ulanov, A. A. Pushkina, M. W. Richards, I. A. Fedorov, and A. I. Lvovsky, Enlargement

- of optical Schrödinger's cat states, *Nat. Photonics* **11**, 379 (2017).
- [54] J. Nunn *et al.*, Theory of noise suppression in Λ -type quantum memories by means of a cavity, *Phys. Rev. A* **96**, 012338 (2017).
- [55] K. Jensen, W. Wasilewski, H. Krauter, T. Fernholz, B. M. Nielsen, M. Owari, M. B. Plenio, A. Serafini, M. M. Wolf, and E. S. Polzik, Quantum memory for entangled continuous-variable states, *Nat. Phys.* **7**, 13 (2011).
- [56] L. Ma, X. Lei, J. Yan, R. Li, T. Chai, Z. Yan, X. Jia, C. Xie, and K. Peng, High-performance cavity-enhanced quantum memory with warm atomic cell, *Nat. Commun.* **13**, 2368 (2022).
- [57] P. Marian and T. A. Marian, Uhlmann fidelity between two-mode Gaussian states, *Phys. Rev. A* **86**, 022340 (2012).
- [58] Y. Takeno, M. Yukawa, H. Yonezawa, and A. Furusawa, Observation of -9 db quadrature squeezing with improvement of phase stability in homodyne measurement, *Opt. Express* **15**, 4321 (2007).
- [59] J. Zhao, H. Jeng, L. O. Conlon, S. Tserkis, B. Shajilal, K. Liu, T. C. Ralph, S. M. Assad, and P. K. Lam, Enhancing quantum teleportation efficacy with noiseless linear amplification, *Nat. Commun.* **14**, 4745 (2023).
- [60] X. Lei, J. Yan, J. Deng, Z. Yan, and X. Jia, High-performance heralded squeezing gate with quantum network modules, *Phys. Rev. A* **110**, 062604 (2024).
- [61] Z. Y. Ou, Efficient conversion between photons and between photon and atom by stimulated emission, *Phys. Rev. A* **78**, 023819 (2008).
- [62] R. Simon, Peres-Horodecki separability criterion for continuous variable systems, *Phys. Rev. Lett.* **84**, 2726 (2000).
- [63] R. F. Werner and M. M. Wolf, Bound entangled Gaussian states, *Phys. Rev. Lett.* **86**, 3658 (2001).
- [64] M. Huo, J. Qin, J. Cheng, Z. Yan, Z. Qin, X. Su, X. Jia, C. Xie, and K. Peng, Deterministic quantum teleportation through fiber channels, *Sci. Adv.* **4**, eaas9401 (2018).
- [65] Y. Yu *et al.*, Entanglement of two quantum memories via fibres over dozens of kilometres, *Nature (London)* **578**, 240 (2020).
- [66] D. Liu *et al.*, Chip-to-chip photonic quantum teleportation over optical fibers of 12.3 km, *Light Sci. Appl.* **14**, 243 (2025).
- [67] Y. Qin, J. Cheng, J. Ma, D. Zhao, Z. Yan, X. Jia, C. Xie, and K. Peng, Efficient and secure quantum secret sharing for eight users, *Phys. Rev. Res.* **6**, 033036 (2024).
- [68] H. S. Stokowski *et al.*, Integrated frequency-modulated optical parametric oscillator, *Nature (London)* **627**, 95 (2024).
- [69] X. Guo, C. R. Breum, J. Borregaard, S. Izumi, M. V. Larsen, T. Gehring, M. Christandl, J. S. Neergaard-Nielsen, and U. L. Andersen, Distributed quantum sensing in a continuous-variable entangled network, *Nat. Phys.* **16**, 281 (2020).